

Asparagus: A Toolkit for Autonomous, User-Guided Construction of Machine-Learned Potential Energy Surfaces

Kai Töpfer^{a,1,*}, Luis Itza Vazquez-Salazar^{a,b,1}, Markus Meuwly^{a,**}

^a*Department of Chemistry, University of Basel, Klingelbergstrasse 80, CH-4056 Basel, Switzerland.*

^b*Present Address: Institute of Theoretical Physics, Heidelberg University, Heidelberg, Germany.*

Abstract

With the establishment of machine learning (ML) techniques in the scientific community, the construction of ML potential energy surfaces (ML-PES) has become a standard process in physics and chemistry. So far, improvements in the construction of ML-PES models have been conducted independently, creating an initial hurdle for new users to overcome and complicating the reproducibility of results. Aiming to reduce the bar for the extensive use of ML-PES, we introduce Asparagus, a software package encompassing the different parts into one coherent implementation that allows an autonomous, user-guided construction of ML-PES models. Asparagus combines capabilities of initial data sampling with interfaces to *ab initio* calculation programs, ML model training, as well as model evaluation and its application within other codes such as ASE or CHARMM. The functionalities of the code are illustrated in different examples, including the dynamics of small molecules, the representation of reactive potentials in organometallic compounds, and atom diffusion on periodic surface structures. The modular framework of Asparagus is designed to allow simple implementations of further ML-related methods and models to provide constant user-friendly

*Corresponding author.

E-mail address: kai.toepfer@unibas.ch

**Corresponding author.

E-mail address: m.meuwly@unibas.ch

¹This authors contributed equally

access to state-of-the-art ML techniques.

Keywords: Machine Learning, Neural Networks, Potential Energy Surfaces

PROGRAM SUMMARY

Program Title: Asparagus

CPC Library link to program files: (to be added by Technical Editor)

Developer's repository link: <https://github.com/MMunibas/Asparagus>

Code Ocean capsule: (to be added by Technical Editor)

Licensing provisions: MIT

Programming language: Python

Supplementary material: Access to Documentation at <https://asparagus-bundle.readthedocs.io>

Nature of the problem(approx. 50-250 words):

Constructing machine-learning (ML) based potential energy surfaces (PESs) for atomistic simulations is a multi-step process that requires a broad knowledge in quantum chemistry, nuclear dynamics and programming. So far, efforts mainly focused on developing and improving ML model architectures. However, there was less effort spent on providing tools for *consistent and reproducible workflows* that support the construction of ML-PES for a variety of chemical systems for the broader science community.

Solution method(approx. 50-250 words):

Asparagus is a program package written in Python that provides a streamlined and extensible workflow with a user-friendly command structure to support the construction of ML-PESs. This is achieved by bundling and linking data generation and sampling techniques, data management, model training, testing and evaluation tools into one modular, comprehensive workflow including interfaces to other simulation packages for the application of the ML-PESs. By lowering the entrance barriers especially for new users, Asparagus supports the generation and adjustment of ML-PESs that allow an increased focus on the physico-chemical evaluation of the chemical system or application in molecular dynamics simulations.

Additional comments including restrictions and unusual features (approx. 50-250 words):

Asparagus is a modular package written in Python providing an underlying structure for further extensions and maintenance. Currently, methods based on message-passing neural network (NN) models using the PyTorch Python package are available. Additions of new models and interfaces to already implemented modules are possible. The NN architecture and hyperparameters are stored in a global configuration module and as a json file for documentation. Except for essential input information, default input parameters are used if not specifically defined otherwise, which allows a quick setup for the construction of a ML-PES but also the fine-tuning for specific needs.

1. Introduction

Potential energy surfaces (PESs) for atomic systems are crucial for investigating the structural and dynamical physico-chemical properties of chemical systems at an atomistic level. Prerequisites for accurate simulations are high-quality and validated representations of the inter- and intramolecular interactions involved. Techniques for constructing such machine-learned potential energy surfaces (ML-PES) - also known as machine-learning potentials¹ - have gained traction over the past decade. Representative approaches are based on permutationally invariant polynomials (PIPs),[1, 2] neural network (NN) techniques as used in SchNet[3], PhysNet,[4] or DeepPot-SE,[5] kernel-based methods, including (symmetrized) gradient-domain machine learning ((s)GDML),[6, 7] reproducing kernel Hilbert spaces,[8, 9, 10] FCHL[11] or Gaussian process regression[12, 13]. The current state-of-the-art of the field was also reviewed continuously[14, 15, 16, 17].

Despite the progress that has been made, constructing and validating ML-PESs suitable for MD or MC simulations can still be a time-consuming and challenging task, particularly if globally robust surfaces are sought. One particularly challenging application is the study of chemical reactions.[18, 16, 19, 20] The process of breaking and forming chemical bonds increases the accessible configurational space that needs to be covered dramatically.

¹Although in the literature it is common to find both names, the present work uses ML-PES instead of MLP to avoid confusion with “multi-layer perceptron”.

On the other hand, this is one of the applications where ML-PESs “shine” as conventional parametrized PESs or more empirical energy functions force fields are either not sufficiently accurate or do not include the possibility of describing chemical reactions, although exceptions exist.[21, 22, 23]

One specific advantage of ML-based techniques is that the inference time of such models is independent of the level of theory at which the reference data - usually from electronic structure calculations - was obtained. Once the reference data are available, the ML-PES is trained and successfully validated, atomistic simulations can be carried out significantly more efficiently and close to the corresponding level of theory, which is particularly relevant for high-level reference methods such as CCSD(T), CASPT2 or MRCI.[24] Concerning inference times, NN-based representations are independent on the size of the training set, whereas kernel-based methods scale $\mathcal{O}(N_{\text{train}}^3)$ with training data set size.[25] On the other hand, NN-based approaches are in general more “data hungry” compared with kernel-based methods in particular, if global and reactive PESs are sought.

Program suites including TorchANI,[26] TorchMD,[27] SchNetPack,[28] FeNNol,[29] MLAtom3,[30] and DeePMD-kit[31, 32] were introduced, which allow training and using machine-learned PES models to run MD simulations with in-built methods or provide interfaces to other modules or programs, such as atomic simulation environment (ASE)[33] or LAMMPS.[34] These programs, however, require at least an initial set of reference training data. In addition, and more relevant to the present work, a new program suite ArcaNN[35] has been recently introduced with the capability of generating the initial training sets from *ab-initio* MD simulations while using DeePMD-kit to handle the ML-PES.

The present work introduces the Asparagus suite that provides Python-based utilities for automating the computational workflow to generate high-dimensional ML-PESs from reference data acquisition, model training and validation up to applications for property predictions. Asparagus provides interfaces to Python packages including ASE[33] and molecular simulation programs such as CHARMM.[36, 37] The present work provides an overview of implemented functionalities and methods together with illustrative application examples including input code for reproduction.

2. Program Overview

Asparagus is a workflow for constructing ML-PESs for given molecular systems. Following the analogy of how an asparagus plant grows, it is noticed that the different steps for constructing an ML-PES are developed independently following a modular fashion. Asparagus is completely written in Python and builds on state-of-the-art tools and the most recent versions of PyTorch[38] and ASE[33].

The modular structure of Asparagus enables additions to cover and include new developments and tools in each module without the need to modify other modules or the parameter pipeline between them. The input parameters for constructing a ML-PES are stored in a global configuration module and written to a json file, which is continuously updated for parameter documentation. The aim is to allow reproducibility of the workflow or recovering the latest state of the model.

Constructing a ML-PES can be divided into several fundamental steps, see Figure 1).[39, 18, 40] The strategies implemented and available in Asparagus are described in the following.

1. **Sampling** Reference structures for an initial ML-PES first need to be generated. This can be accomplished with the various sampling methods implemented in Asparagus, or such samples can be imported from a pre-existing reference data source. Asparagus also supports the reference property computation of the sample structures with methods at a user-defined level of theory. In particular, the interface between Asparagus and ASE supports calculators for quantum chemical programs such as ORCA[41] or Gaussian[42] but can also be extended to other such programs. It also provides reference calculation schemes including empirical energy functions, density functional theory (DFT) and higher level *ab initio* methods based on preparing and running customizable template files to provide flexibility. The molecular structures and its reference properties, including energy, atomic forces, atom charges, and molecular dipoles, are stored in a Asparagus style database file in different formats, including SQL (default), HDF5 or Numpy npz.

2. **Training** The database format implemented in `Asparagus` provides the information required for training an ML-PES. The reference data are split into a training, validation, and testing data subsets. The loss function needs to be defined, and a PyTorch optimizer is initialized, either from the default settings or through user-specific input. Currently, `Asparagus` is linked to the PhysNet[43] and PaiNN[44] NN architectures. The modular approach of `Asparagus`, however, allows for the straightforward addition of further established ML architectures such as SchNet[45], Nequip[46], or MACE[47]. Within the capabilities of the PyTorch module, the training procedure can be executed on the CPU or GPU. During training, the best model parameter set is stored according to the lowest loss value for the property prediction of the validation dataset.
3. **Testing** `Asparagus` provides functions to evaluate the accuracy of property predictions (see **Sampling** above) for the complete reference dataset or its subsets. This module returns statistical measures such as mean absolute error (MAE) and root-mean squared error (RMSE) for each reference property. It is also possible to generate various correlation plots (reference vs. predicted property, reference vs. prediction error) or prediction error histograms. During model training, if a new best model parameter set is found at the model validation, the mentioned test functions are executed for the test data subset by default.
4. **Characterization** `Asparagus` includes native tools to determine important characteristics of a ML-PES. These tools allow searching for a minimum energy path or minimum dynamic path[48] along the PES between two reactant states. A diffusion Monte-Carlo (DMC) method is implemented for the search of regions in the PES undersampled within the reference dataset.[49, 50, 51, 52]. The ML-PES is available as an ASE calculator and can be used through ASE to determine, e.g. harmonic frequencies. This function can be used to further validate the accuracy and stability of the ML-PES or to identify regions in configurational space which require additional samples. In the latter case, these regions can be additionally sampled; the data is added to the reference dataset and used to refine the ML-PES.[37]
5. **Interfaces** As already mentioned, the ML-PES can be loaded as an

ASE calculator object and used for ASE functionalities such as MD simulations. Alternatively, MD simulations can be carried out through an interface between `Asparagus` and the CHARMM suite of codes through the `MLpot` module of the `pyCHARMM` API (see section 4).[53, 36] This enables MD simulations using a) the ML-PES for the energy and force evaluation of a system or b) ML/MM simulations using mechanical embedding of the ML-PES and the `CGenFF` force field[54] in CHARMM, e.g., for simulation of a molecule (ML) in solution (MM).[55]

3. Program Features

As summarized in Section 2, `Asparagus` functions can be divided into five main classes: sampling, training, testing, characterization and interfaces. A schematic overview of the functions and their interdependencies is shown in Figure 1. In the following, the capabilities of each class are described in more detail. Further information can be found in online documentation (<https://asparagus-bundle.readthedocs.io/>).

3.1. Sampling

Sampling the configurational space is a key step for constructing an ML-PES since the task is to deduce a functional form of the PES purely from data.[39, 40] Nevertheless, an exhaustive sampling of the configuration space is usually unfeasible because of the exponential scaling of the size of configurational space, in particular for applications to chemical reactions. Additionally, the computational cost of quantum chemical calculations also scale exponentially with the number of electrons, which becomes computationally significant when high-level methods such as `CCSD(T)` or multi-reference methods including `CASPT2` or `MRCI`, are applied.

There are multiple strategies to perform the initial sampling of an atomic system. In `Asparagus`, some of the most commonly used methods are implemented, including molecular dynamics (MD), Monte-Carlo (MC), normal mode sampling (NMSamp), and metadynamics (Meta). Additionally, an alternative to NMSamp is available, which is referred to as normal mode scanning (NMScan). The implementation of the sampling methods makes extensive use of ASE. Therefore, other initialized ASE optimizer or propagator objects, such as for nudged elastic band (NEB)[56], minima hooping[57],

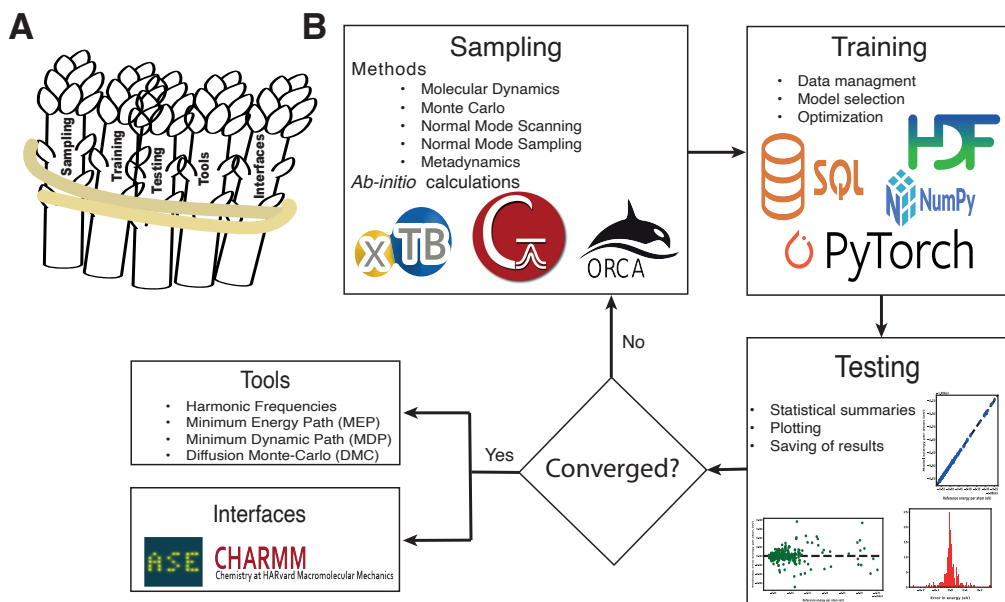


Figure 1: Scheme representation of the `Asparagus` classes (panel A) and a workflow chart (panel B) that represents class details and procedures for the construction of a ML-PES in `Asparagus`.

or basin hopping[58] can be passed to `Asparagus` to run and store the reference data.

By default, `Asparagus` uses the ASE interface of the `xTB`[59] calculator to compute initial reference properties. This tight binding density functional method GFN2-`xTB` is fast and convenient but will not provide accurate reference properties for training a ML-PES. Still, it is useful for test purposes of the command pipeline. For high-level results, ASE calculators connecting to *ab-initio* codes such as ORCA, MOLPRO,[60] or Gaussian should be used. The following provides background on the sampling methods implemented in `Asparagus`.

Molecular Dynamics and Monte-Carlo. Molecular Dynamics (MD) or Monte-Carlo (MC) simulations are the most common methods to generate initial databases to construct a ML-PES. For MD simulations, the Newtonian equations of motion are propagated in time to explore the configuration space of

a chemical system. The given temperature T will not only define the average kinetic energy of the system but also determine the magnitude of deformations of the atomic systems conformations. This also affects the possibility of overcoming reaction barriers that yield sampling of a larger configuration space. Usually, the sampling of the chemical system should be carried out at a higher temperature than that envisaged for the production simulations. This ensures that the ML-PES does not enter the extrapolation regime during simulations for which especially NN-based PESs cannot guarantee accurate property predictions.[40, 18]

Although MD is commonly used for the initial sampling of PESs for ML models, it has some disadvantages, such as the correlation between the generated structures and a negligible probability of sampling rare events (i.e. reactive systems).[18] Therefore, MD should be used in simulations close to equilibrium that do not involve rare events.[18] In *Asparagus*, MD sampling is implemented using Langevin dynamics, where the temperature of the system is kept constant by adding a fluctuating force and a friction term is used to emulate the presence of a heat bath.

On the other hand, MC sampling is a method where the configuration space \mathbf{x} is explored by random atom displacements.[24] The MC method generates random single-atom displacements \mathbf{x}' with respect to a uniform distribution. The new position is accepted if the energy difference of the system $\Delta E = E(\mathbf{x}') - E(\mathbf{x})$ in the form of $a = \exp(-\Delta E/k_b T)$ is smaller than a random value $c = [0, 1]$ of uniform distribution. The acceptance criteria a can be modulated by changing the sampling temperature. This implementation is known as the Metropolis-Hastings (MH) algorithm.[61] The MH algorithm is commonly used in molecular simulations and implemented in *Asparagus*. In general, MC has the advantage over MD in that MC does not require any forces.[62]

Normal Mode Sampling. Normal mode sampling (NMSamp) is an alternative to MD-based sampling and allows targeted characterization of relevant regions of a PES.[63, 40] Using the vibrational normal mode vectors $\mathbf{Q} = \mathbf{q}_i$ obtained from harmonic analysis of a molecule in an equilibrium conformations \mathbf{x}_{eq} , NMSamp generates new sample conformations \mathbf{x}_n in a random fashion by applying all N_ν normal mode vectors, each scaled by a factor

$f_i(c_i, k_i, T)$

$$\mathbf{x}_n = \mathbf{x}_{\text{eq}} + \sum_i^{N_\nu} f_i(c_i, k_i, T) \mathbf{q}_i \quad (1)$$

applied to the equilibrium conformation. The displacement scaling factor

$$f_i = \pm \sqrt{\frac{3c_i k_b T}{k_i}} \quad (2)$$

depends on the random number $c_i \in [0, 1]$, the force constant k_i of the respective normal mode i , temperature T , and k_b is the Boltzmann constant. The sign of f_i is determined randomly from a Bernoulli distribution with $P = 0.5$. The procedure is repeated until the desired number of samples has been generated.

NMSamp generates uncorrelated conformations in an efficient manner. However, the sampling is based on the harmonic approximation around the minimum energy structure. NMSamp can also be combined with other techniques, such as NEB, to sample regions along a specific path in the PES, which becomes particularly convenient for reactive systems.[64]

Normal Mode Scanning. Normal mode scanning (NMScan) is a sampling algorithm that generates atom displacements along scaled vibrational normal mode vectors $\mathbf{Q}_\nu = \{\mathbf{q}_i\}$ on the initial conformation \mathbf{x}_{init} for which the harmonic frequencies ν and normal modes have been computed. The algorithm iterates over a specified combination of normal modes and applies a normal mode vector (or combination of normal mode vectors) scaled by negative and positive multiples n of a frequency-dependent scaling factor f_i . The scaling factor f_i is determined by a user-defined input E_{step} . Within the harmonic approximation, the energy step size E_{step} is supposed to match the energy difference $\Delta E_{i,n=\pm 1}(f_i)$

$$E_{\text{step}} = \Delta E_{i,n=\pm 1}(f_i) = |E(\mathbf{x}_{\text{init}} \pm f_i \mathbf{q}_i) - E(\mathbf{x}_{\text{init}})| \quad (3)$$

between the initial energy $E(\mathbf{x}_{\text{init}})$ and the energy when the respectively scaled normal mode vector is applied once $E(\mathbf{x}_{\text{init}} \pm f_i \mathbf{q}_i)$. Positive and negative multiples of the scaled normal mode vector ($n f_i \mathbf{q}_i$ with $n \in \mathbb{Z}$) are applied until the absolute energy difference $\Delta E_{\nu,n}$

$$\Delta E_{i,n} = |E(\mathbf{x}_{\text{init}} + n f_i \mathbf{q}_i) - E(\mathbf{x}_{\text{init}})| \quad (4)$$

reaches a user-defined energy limit E_{limit} or the absolute value of the multiplier $|n|$ reached a user-defined step limit n_{max} .

The normal mode scaling factor f_i for each frequency ν_i depends on their respective force constant k_i

$$k_i = 4\pi^2(c\nu_i)^2/\mu_i \quad (5)$$

where c is the speed of light and μ_i is the reduced mass of the respective normal mode

$$\mu_i = \left[\sum_j^{N_{\text{atoms}}} (\mathbf{q}_i \cdot \mathbf{q}_i) / m_j \right]^{-1} \quad (6)$$

with m_j the atom mass of atom j . The normal modes are each normalized by $\mathbf{q}_i = \mathbf{q}'_i / \|\mathbf{q}'_i\|$ with \mathbf{q}'_i as the normal mode vector from the harmonic vibrational analysis. According to the harmonic approximation for the potential along the scaled normal mode vector $f_i \mathbf{q}_i$ with

$$E_i(f) = 0.5k_i \cdot \|f\mathbf{q}_i\|^2 = 0.5k_i \cdot f^2 \quad , \quad (7)$$

the respective scaling factor f_i to yield E_{step} is

$$f_i = \sqrt{\frac{2E_{\text{step}}}{k_i}}. \quad (8)$$

It is important to mention that the real initial energy difference ($n = \pm 1$) will not yield the defined energy step value E_{step} due to the anharmonicity of the PES and will not change proportional to $\propto n^2$ for increasing n . Depending on the atomic system and vibrational mode, the real energy steps can both propagate less strongly (e.g. bond dissociation of a diatomic molecule) or more strongly (e.g. bending modes of larger molecules). It is, therefore, not possible to predict the exact number of steps computed along the scan path until the energy limit is reached.

The initial conformation \mathbf{x}_{init} on which the harmonic normal mode analysis is applied does not necessarily have to be an equilibrium structure. Even for structures exhibiting one (transition state) or multiple imaginary frequencies, the algorithm handles the normal modes as usual until the energy difference $\Delta E_{i,n}$, defined as absolute value reaches the energy limit or step limit.

As mentioned, normal mode scanning can be applied to a combination \mathbf{C} of a number of multiple normal modes N_C , that yields an expression for the energy difference

$$\Delta E_{\mathbf{C},\mathbf{n}} = |E(\mathbf{x}_{\text{init}} + \sum_{i,i \in \mathbf{C}}^{N_C} n_i f_i \mathbf{q}_i) - E(\mathbf{x}_{\text{init}})| \quad (9)$$

with multipliers $\mathbf{n} = \{n_i\}$. However, iterating over all possible combinations of normal modes lead to a large number of new conformations, which can become excessive for larger molecules. In practice, it may be advantageous to apply a scan over a combination of a subset of normal modes with, e.g., frequencies in a certain range of wave numbers.

Metadynamics. Metadynamics is a technique that allows the acceleration of sampling rare events and the estimation of the free energies of complex atomic systems.[65, 66] This is achieved by introducing a history-dependent bias potential based on a number N_{cv} of collective variables (CVs) denoted as $\mathbf{S} = \{s_i\}$. In general, a CV can be any of the degrees of freedom of the system.[67, 68, 69] In Asparagus currently supported CVs are bond distances, bond angles, dihedral angles or reactive coordinates (e.g. difference between two bond distances) between atoms. The choice of CVs crucially affects the effectiveness of metadynamics to yield reliable free energy surfaces for rare events.[66] For conformational sampling the selection of CVs is less critical as their choice should just provide sufficient coverage of the structures along the “reaction” path.[18, 68, 70]

In practice, Metadynamics simulations are MD (or MC) simulations on a PES $V(\mathbf{x})$ that is perturbed by a “bump” potential V_{bump} to gradually fill the basins of $V(\mathbf{x})$. V_{bump} is a sum of N_α Gaussians

$$V_{\text{bump}} = \sum_{\alpha}^{N_\alpha} G(\mathbf{S}, \mathbf{S}_\alpha) = \sum_{\alpha}^{N_\alpha} \lambda \exp \left(- \sum_i^{N_{\text{cv}}} (s_i - s_{i,\alpha})^2 / (2\sigma_i^2) \right) \quad (10)$$

each centered around CV coordinates \mathbf{s}_α with Gaussian height λ and width $\boldsymbol{\sigma} = \{\sigma_i\}$. The number of Gaussians N_α increases by one at each user-defined interval of the simulation with a new set of \mathbf{S}_α at the current frame.

Usually, the combination of Gaussian heights λ and widths σ is chosen small enough to keep the system in close to thermodynamic equilibrium but sufficiently large to achieve efficient sampling of the free energy surface.[66] For the purpose of conformation sampling, keeping the thermodynamic equilibrium is less relevant and large λ and σ values yield rapid sampling of the configuration space. The consequently large increase in the simulation temperature is countered by a high friction coefficient of the applied Langevin thermostat. For that reason, the implemented sampling algorithm is called meta-sampling rather than -dynamics.

3.2. Training and Testing

The reference data used for training and testing of the ML-PES are stored in the Asparagus database file. The database class of Asparagus is inspired by the database class implemented in ASE, providing a minimalist version to store, update and supply data. It is designed to allow data to be stored in different file formats such as SQL (via sqlite3 python package), HDF5 (via h5py python package), or .npz (compressed numpy format) format. Reference data can be read from all Asparagus database formats and formats such as ASE database files, ASE trajectory files and Numpy npz files.

The database entries contain general information on atom types, positions and the system’s total charge. Additionally, support for periodic systems is provided by storing boundary conditions in each Cartesian direction and cell parameters. Asparagus provides the “quality-of-life feature” to internally handle unit conversion between different reference datasets according to the defined property units. It will also handle the conversion between reference property units and different model property units during the model training if needed. By default, ASE units will be used, i.e. positions in Å and energies in eV.

If not specifically defined, the default settings and hyperparameters are used for the training procedure. By default, the reference data are split into 80% for the training, 10% for validation, and 10% for testing. The loss function for parameter optimization is

$$\mathcal{L} = W_E \mathcal{L}_E(E_{\text{ref}}, E_{\text{pred}}) + W_F \mathcal{L}_F(F_{\text{ref}}, F_{\text{pred}}) + W_D \mathcal{L}_D(D_{\text{ref}}, D_{\text{pred}}) + W_Q \mathcal{L}_Q(Q_{\text{ref}}, Q_{\text{pred}}) \quad (11)$$

Here, the weights $W \in [E, F, D, Q]$ for the properties energy E , forces F , molecular dipole D and atomic charges Q are defined as $W_E = 1$, $W_F = 50$, $W_D = 25$ and $W_Q = 1$. The smooth L1 loss function \mathcal{L} is defined as:

$$\mathcal{L}(x_{\text{ref}}, x_{\text{pred}}) = \begin{cases} 0.5 \cdot \frac{(x_{\text{ref}} - x_{\text{pred}})^2}{\beta} & \text{If } |x_{\text{ref}} - x_{\text{pred}}| < \beta \\ |x_{\text{ref}} - x_{\text{pred}}| - 0.5 \cdot \beta & \text{else} \end{cases} \quad (12)$$

where $\beta = 1$, although it can be adjusted by the user. Also, the user can define other functional forms for the loss function. By default, Asparagus uses the AMSGrad variant of the Adam algorithm[71, 72] with a learning rate of 0.001, a weight decay of 10^{-5} , and an exponential learning rate scheduler with a decay rate of 0.999. All optimization algorithms and learning rate schedulers implemented in PyTorch are available. To avoid overfitting, early stopping,[73] exponential moving average with a decay of 0.99, and a gradient clipping function are implemented. The training is performed in epochs with a validation step every n th epoch ($n = 5$ by default). Checkpoint files of the model parameter state are stored for the model at the last validation step, and each time a new best-performing validation loss value is reached.

After training, each best model state is evaluated on the test data. Asparagus computes statistical quantities including MAE, RMSE and the Pearson correlation coefficient ($1 - r^2$) for each property of the loss function. The performance of the trained model is graphically represented as (x/y) -correlation plots between reference values (x) and property prediction (y) and reference values, prediction error and histograms of prediction error.

3.3. Tools

Once an ML-PES has been obtained, standard properties that characterize it can be determined. In Asparagus, suitable tools have been implemented, which are briefly described in the following. It should be noted, however, that other quantities than those discussed next may be of interest to the user, depending on the project at hand.

Minimum Energy Path. The MEP is defined as the lowest path energy connecting reactants and products by passing through the transition state. The MEP is obtained by following the negative gradient of the PES starting from

the transition state along the normal coordinate of the imaginary frequency. Usually, this is done by integrating the path in small steps (ϵ) using the Euler method, which updates the positions as:

$$\mathbf{x}_{n+1} = \mathbf{x}_n - \epsilon \nabla V(\mathbf{x}_n) ; \mathbf{x}_0 = \mathbf{x}_{TS} \quad (13)$$

Minimum Dynamic Path. Complementary to the minimum energy path is the minimum dynamic path (MDP),[48] which provides information about the lowest path between reactants and products in phase space. In this case, Newton’s equation of motion is integrated over the normal coordinate of the imaginary frequency of the TS for small time steps (ϵ) using the velocity Verlet scheme[74]. This formulation keeps information about the previous gradients in the velocities. Then, the positions and velocities are obtained as:

$$\mathbf{x}_{n+1} = \mathbf{x}_n + \epsilon \mathbf{v}_n - \frac{1}{2m} \nabla V(\mathbf{x}_n) ; \mathbf{x}_0 = \mathbf{x}_{TS} \quad (14)$$

$$\mathbf{v}_{n+1} = \mathbf{v}_n - \frac{\epsilon}{2m} (\nabla V(\mathbf{x}_n) + \nabla V(\mathbf{x}_{n+1})) ; \mathbf{v}_0 = 0 \quad (15)$$

Diffusion Monte Carlo. DMC is based on the similarity between the diffusion equation with a sink term and the imaginary-time Schrödinger equation (replace $t \rightarrow -i\tau$) with an energy shift term.[50] Then, random-walk simulations can be used to solve it and to obtain the quantum mechanical zero-point energy (ZPE) and nuclear ground-state wavefunction of a molecule[75, 76, 49]. During a DMC simulation, the atoms are randomly displaced, allowing an efficient exploration of conformational space. Therefore, the DMC method can be used to detect holes (i.e. regions on a PES that have large negative energies with respect to the global minimum) in ML-PESs.[51] Asparagus uses DMC for this purpose.

The method is formulated as follows. For a system of interest, a set of walkers - their ensemble is a proxy for the nuclear wavefunction - is initialized at x_0 . The walkers are then randomly displaced at each time step τ according to

$$\mathbf{x}_{\tau+\Delta\tau} = \mathbf{x}_\tau + \sqrt{\frac{\hbar\Delta\tau}{m}} r \quad (16)$$

where \mathbf{x}_τ corresponds to coordinates at time step τ , $\Delta\tau$ is the time step of the random-walk simulation, m is the atomic mass, and r is a random

number drawn from a Gaussian distribution, $\mathcal{N}(0, 1)$. The walkers obtained from Equation 16 are then used to compute the potential energy (E_i) of each walker i . In the next step, the potential energies of the walkers are compared with a reference energy E_r , to determine whether a walker stays alive, gives birth to a new walker or is killed. The probabilities of birth or death of walker are given by

$$P_{\text{death}} = 1 - e^{-(E_i - E_r)\Delta\tau} \quad (E_i > E_r) \quad (17)$$

$$P_{\text{birth}} = e^{-(E_i - E_r)\Delta\tau} - 1 \quad (E_i < E_r) \quad (18)$$

After the probabilities are obtained, the walkers that do not pass the threshold are removed, and new walkers are born. As a consequence of the dead-birth process, the number of alive walkers fluctuates. Next, E_r is adjusted according to

$$E_r(\tau) = \langle V(\tau) \rangle - \alpha \frac{N(\tau) - N(0)}{N(0)}. \quad (19)$$

The averaged potential energy of the alive walkers is given by $\langle V(\tau) \rangle$, α is a constant/parameter that governs the fluctuation in the number of walkers and the reference energy, and $N(\tau)$ and $N(0)$ are the number of alive walkers at time step τ and 0, respectively.

4. Examples of Use

In the following, representative applications are described. The first example is discussed in more detail together with sample code, whereas the second and third examples are more illustrative of the capabilities of *Asparagus*.

4.1. Conformational Sampling in the Gas Phase and in Solution: Ammonia Conformations for ammonia (NH_3) were sampled by different sampling methods implemented in *Asparagus* and used to train a ML-PES using PhysNet to show the capabilities and limitations of the sampling methods and their impact on a trained ML-PES. The performance of the models was evaluated by the RMSE between model and reference properties, bond elongation potentials, vibrational harmonic frequencies and simulation results of single ammonia in water using a QM(ML-PES)/MM approach with mechanical embedding.

ML-PESs were trained using Asparagus and different reference data for a single ammonia molecule sampled by (A) MD simulation at 500 K (Listing 1), (B) Metadynamics sampling (Listing 2) at 500 K with each N-H bond assigned as CV, and (C) normal mode scanning along single (Listing 3) and permutations of two normal mode vectors. By providing an initial guess of the ammonia structure (e.g. via a *.xyz* file), all sampling methods were initialized and started by a single Python command, respectively.

```

1 from asparagus.sample import MDSampler
2 sampler = MDSampler(
3     sample_systems='nh3_c3v.xyz',
4     sample_calculator='ORCA',
5     sample_calculator_args = {
6         'orcasimpleinput': 'RI PBE D3BJ def2-SVP def2/J'},
7     md_temperature=500, # K
8     md_time_step=1.0, # fs
9     md_simulation_time=10_000.0, # fs
10    md_save_interval=10,
11    )
12 sampler.run()

```

Listing 1: Input for MD sampling of NH₃ at 500 K producing 1000 reference samples

```

1 from asparagus.sample import MetaSampler
2 sampler = MetaSampler(
3     sample_systems='nh3_c3v.xyz',
4     sample_calculator='ORCA',
5     sample_calculator_args = {
6         'orcasimpleinput': 'RI PBE D3BJ def2-SVP def2/J'},
7     meta_cv=[[0, 1], [0, 2], [0, 3]], # N(0)-H(1,2,3)
8     meta_gaussian_height=0.05, # eV
9     meta_gaussian_widths=0.1, # Angstrom
10    meta_gaussian_interval=10,
11    meta_temperature=500, # K
12    meta_time_step=1.0, # fs
13    meta_simulation_time=10_000.0, # fs
14    meta_save_interval=10,
15    )
16 sampler.run()

```

Listing 2: Input for metadynamics sampling of NH₃ with the 3 N-H bonds as collective variables producing 1000 reference samples

```

1 from asparagus.sample import NormalModeScanner
2 sampler = NormalModeScanner(

```

```

3     sample_systems='nh3_c3v.xyz',
4     sample_calculator='ORCA',
5     sample_calculator_args = {
6         'orcasimpleinput': 'RI PBE D3BJ def2-SVP def2/J'},
7     nms_harmonic_energy_step=0.05, # eV
8     nms_energy_limits=1.00, # eV
9     nms_number_of_coupling=2,
10    )
11 sampler.run(nms_frequency_range=[('>', 100)]) # modes > 100cm-1

```

Listing 3: Input for normal mode scanning of NH₃ along single and a combination of two normal modes that produces 1595 reference samples

The sampling methods generated 1000 (method A), 1000 (B) and 1595 (C) structures for which reference data (energies, forces, dipole moments) was generated at the PBE-D3/def2-SVP level using ORCA.[41] As indicated above, the final number of samples generated by normal mode scanning can not be predicted *a priori*. Hence, the difference between the number of samples between methods A/B and C.

```

1 from asparagus import Asparagus
2 model = Asparagus(
3     config='config.json', # File path to store model parameters
4     data_file='data.db', # Respective reference database
5     model_type='physnet', # Default ML-PES
6     model_properties=['energy', 'forces', 'dipole'],
7 )
8 model.train(trainer_max_epochs=1_000)
9 model.test(test_datasets='all')

```

Listing 4: Input for PhysNet model training and final evaluation on all datasubsets

```

1 from asparagus import Asparagus
2 from ase import io
3 model = Asparagus(config='config.json')
4 calc = model.get_ase_calculator()
5 ammonia = io.read('nh3_c3v.xyz', format='xyz')
6 ammonia.calc = calc
7 ammonia.get_potential_energy()
8 # ... model potential evaluation

```

Listing 5: Input for PhysNet model evaluation by reading parameters from the configuration file and loading the ASE calculator interface

The PhysNet ML-PESs were trained on energies, forces and molecular dipole moments for at most 1000 epochs (sufficient for convergence) using the in-

put code in Listing 4 for each of the sampled reference data sets A to C. Average RMSEs per conformation and atoms for the energies (forces) on the test sets were (A) 4.1 meV (45.4 meV/Å), (B) 7.4 meV (59.3 meV/Å) and (C) 7.3 meV (48.5 meV/Å). As judged from the RMSE values, the PES trained on (B, metadynamics) performs worst for both energy and forces. On the other hand, this data set covered the widest range of potential energies compared with A or C, respectively, see Figure 2B. Further evaluations were performed by using ASE and the ASE calculator interface of the model potential; see Listing 5.

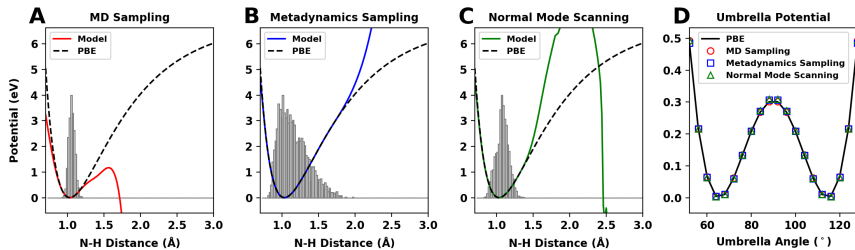


Figure 2: Bond potential for a single N-H bond elongation in ammonia predicted by the PBE reference method (dashed black line) and PhysNet model potentials trained on reference data from (A) MD simulation, (B) metadynamics and (C) normal mode scanning sampling methods. The hollow grey bars indicate N-H bond distance distribution in the respective data sets. Panel D shows the potential curve along the umbrella motion in ammonia predicted by the PBE reference method (dashed black line) and the PhysNet model potentials trained on reference data from MD simulation (red line), metadynamics (blue dash-dotted line) and normal mode scanning sampling methods (green dotted line).

The advantage of sampling wider energy ranges can be seen in the stretch potential of a single N-H bond of ammonia away from the equilibrium conformation; see Figure 2. Predictions for the ML-PES trained on (B, metadynamics data) remain at least qualitatively correct for N-H bond lengths up to 1.7 Å and 3 eV above the minimum energy. For the curves in Figures 2A and 2C the predictions start to differ significantly from the reference potential at even smaller bond elongation away from the equilibrium distance because larger distances were not sufficiently covered in the reference data sets.

For energy predictions along the umbrella motion in ammonia ($C_{3v} \rightarrow D_{3h} \rightarrow C_{3v}$), see Figure 2D, the PhysNet model trained on MD data (A) predicts

closest to the reference energy difference between equilibrium and transition state potential with an error of 0.15 meV. Barrier heights for the ML-PESs trained on metadynamics sampling (B) and normal mode scanning data (C) deviate by 5.04 meV and 6.84 meV, respectively, which were also found to fluctuate more within a set of independently trained models following the same workflow. The energy RMSEs in a set of independently trained models on MD data remain narrowly small. This may indicate an insufficient number of samples in the metadynamics and NMS datasets with respect to the range of the sampled configurational space or the potential energy range, which is required for a well-trained and converged PhysNet model.

Validation with respect to harmonic frequencies of the six vibrational normal modes are considered next. The RMSE per normal mode between the reference frequencies at the PBE level of theory and the model frequencies are lowest (16.0 cm^{-1}) for the model trained on NMS data. ML-PESs trained on metadynamics sampling and MD data yield an RMSE per normal mode of 31.6 cm^{-1} and 53.8 cm^{-1} , respectively. These differences indicate that further improvements can be achieved by either adding additional samples around the global minimum, more extensive training, or both. The model trained on metadynamics data performs better for the higher N-H stretch mode frequencies but worse for the lower bending mode frequencies compared with the MD-data trained model.

```

1 import pycharmm
2 from asparagus import Asparagus
3 from ase import io
4 # ... initialize simulation system and parameters
5 ml_model = Asparagus(config='config.json')
6 ammonia = io.read('nh3_c3v.xyz', format='xyz')
7 calc = pycharmm.MLpot(
8     ml_model,
9     # atomic numbers of ammonia: [7, 1, 1, 1]
10    ammonia.get_atomic_numbers(),
11    # segment name of ammonia: 'AMM1'
12    pycharmm.SelectAtoms(seg_id='AMM1'),
13    ml_charge=0, # total charge 0 (default)
14    ml_fq=True) # use fluctuating model charges (default)
15 # ... continue with further simulation commands

```

Listing 6: Extraction of the PyCHARMM script to activate the QM(ML)/MM potential representation for ammonia

Asparagus also provides an interface between PhysNet and the CHARMM simulation program via the pyCHARMM API.[53, 36] A trained ML-PES using the PhysNet architecture predicts the required forces and atomic charges, which are required for MD simulations and an electrostatic interaction potential between the conformationally fluctuating NH_3 charges and static atomic point charges as defined by empirical force fields such as CGenFF.[54] Mechanically embedded QM(ML)/MM simulations of ammonia (ML) in TIP3P water solvent (MM) were performed. The necessary van-der-Waals parameters for the NH_3 molecule were those from CGenFF.[77, 36] Here, NVT heating simulation and NPT equilibration simulations of a single ammonia solute in 933 water solvent molecules was performed for 50 ps each followed by a 50 ps NVE simulation to check total energy conservation (Figure 3A) and simulation of and NPT ensemble at 300 K and normal pressure for 100 ps with an MD-time step of $\Delta t = 0.25$ fs. Listing 6 shows an extraction from the pyCHARMM script where an Asparagus potential model is assigned. It is to be mentioned that this simulation setup of the strong base ammonia in water without allowing proton transfer ($\text{NH}_3 + \text{H}_2\text{O} \rightleftharpoons \text{NH}_4^+ + \text{OH}^-$) is chemically inaccurate and only serves as a demonstration.

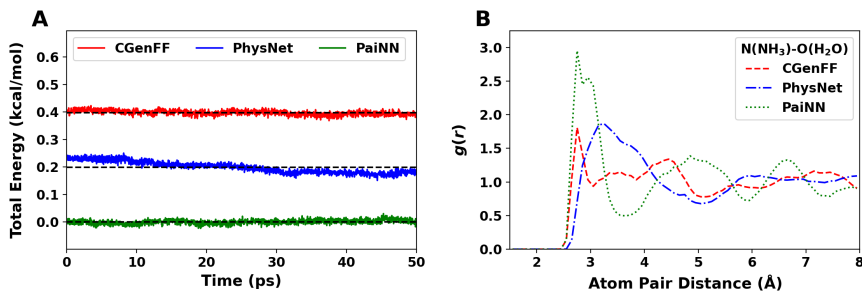


Figure 3: Panel A: Total energy sequence of a NVE simulation for ammonia in water using the classical force field CGenFF and the QM(ML)/MM approach with a trained PhysNet or PaiNN model of ammonia trained on metadynamics sampled data (see Listing 2). The energies are arbitrarily shifted for a better comparison and the dashed black line marks the average energy, respectively. Panel B: Radial distribution function between ammonia’s nitrogen and water oxygen atoms in NpT simulation using different potential models.

Figure 3A shows that the total energy is conserved and only fluctuates with the same magnitude than in the NVE simulations using the empirical CGenFF model (red line). The total energy sequence from simulations using

the PhysNet model potential (blue line) shows a slow oscillation around the energy average but still within reasonable bounds. In addition, a PaiNN[44] ML-PES was trained on the metadynamics data (B). Even though the forces RMSE of the PaiNN model with 24.5 meV/Å is lower than the PhysNet model (59.3 meV/Å), this is not of concern here. Energy conservation is also observed in *NVE* simulations using the PaiNN ML-PES (green line). Figure 3B shows the radial distribution functions ($g(r)$) between the nitrogen atom of ammonia and the oxygen atoms of the water solvent computed from the *NpT* production simulation. The significant difference is caused by the different atomic charge distribution of the neutrally charged ammonia. Within the CGenFF model, the nitrogen and hydrogen atoms of ammonia are assigned static point charges of $-1.125e$ and $0.375e$, respectively. In comparison, the trained PhysNet model predicts for ammonia in C_{3v} equilibrium geometry atomic charges of $-0.964e$ and $0.321e$, whereas the trained PaiNN model predicts $-1.596e$ and $0.532e$.

4.2. Chemical Reactions: Organometallic Complex

To illustrate the capabilities of Asparagus to mix different sampling methods for constructing a PES and its use in the study of a reactive process, the hydrogen transfer step for the hydroformylation catalytic cycle of alkenes using a simplified version of the Wilkinson catalyst with cobalt ($\text{CoH}(\text{PMe}_3)_2(\text{CO})$) was considered.[78] The training data for the reactive step of interest was obtained by determining the reaction path between intermediates taken from Ref. 79 with the NEB method. For generating the training data, electronic structure calculations were carried out at the PBE0/def2-SVP level including D3BJ dispersion corrections using the ORCA code.[41] Subsequently, for each image along the NEB path, normal mode scanning for all modes with frequencies larger than 100 cm^{-1} was performed. The total number of structures thus generated was 3069, which was split into 80 % for training, 10 % for validation and 10 % for testing. A PhysNet model was trained for 1000 epochs using a batch size of 32. Using the obtained model, the minimum energy path using NEB and the minimum dynamic path were determined.

The obtained ML-PES has RMSEs of 1.1 kcal/mol for the energies (Figure 4A), 1.7 kcal/(mol Å) for the forces, and 0.1 D for the dipole moment in the test set. These results are near chemical accuracy for energies and forces,

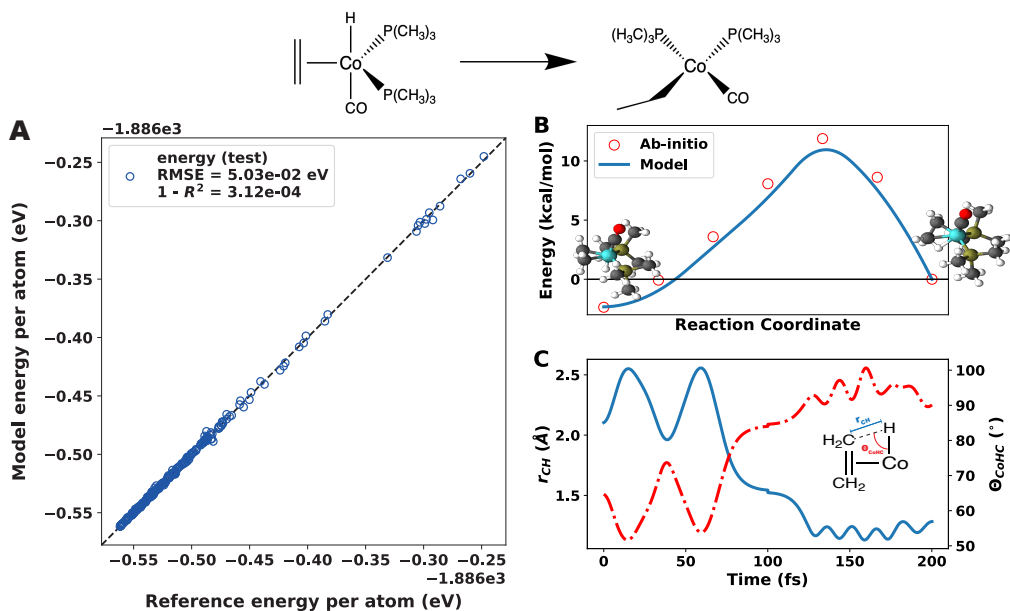


Figure 4: Organometallic reaction. Panel A shows the correlation plot for the prediction energy in the test subset. Panel B displays the minimum energy path obtained from *ab initio* calculations and, with the NN model, insight the panel structures of the equilibrium structures. Complementary panel C shows the change in the distance between the carbon in the alkene and the hydrogen atom bonded to the metal, as well as the angle between the C-H-Co atoms.

indicating a good performance of the fitted model. Further improvements of this ML-PES by increasing the number of samples or using a different NN architecture are, of course, possible. The layout of the graphics shown in Figure 4A is automatically generated by Asparagus at the end of the test procedure for the mentioned quantities. On request, `.csv` and `.npz` files are also generated for each property, which includes columns of reference and predicted values.

Next, the MEP and MDP were determined using the tools implemented in Asparagus. Figure 4B compares the MEP obtained from *ab initio* calculations (red circles) with that from the fitted ML-PES (blue line). A good agreement between the two is found, with a slight underestimation of the energies by the ML model. The calculated MDP on the ML-PES, see Figure 4C, provides chemical insight into the reactive process: as the distance be-

tween the alkene C-atom and the H-atom attached to the Co-atom decreases, a CH-bond (blue trace) is formed. Concomitantly, the C-H-Co angle θ_{CoHC} (red dot-dashed line) changes. Initially, $\theta_{\text{CoHC}} \sim 60^\circ$ because the hydrogen atom is closer to the metallic centre. As the reaction progresses, the alkene rotates to a position where the H bond is perpendicular to the Co and C atoms.

4.3. Handling Periodic Systems: Surfaces

Asparagus also supports the training of ML-PESs for periodic systems such as solids and surfaces. As an example, a PaiNN model is trained to predict energies and forces of the diffusion motions of a gold atom on an Al(100) surface. Reference data were obtained with the GPAW[80] program package using the PBE density functional and a projected augmented wave basis with an energy cutoff at 200 eV. Energies and forces were computed with a k -points grid of (4,4,1) with an Al(100) unit cell of size $2 \times 2 \times 3$ and 4 Å vacuum level. As this is only an illustration, the computational setup was neither optimized nor checked for convergence. Rather, the computational setup was taken from the surface diffusion tutorial reported by ASE[81] and GPAW.[82]

Reference data was obtained from NMS along the normal modes of the gold atom and the four aluminum atoms of the top surface layer at equilibrium conformations of gold at the hollow, bridge and top site of the Al(100) surface. This yielded 5605, 6404 and 6254 reference conformations, respectively. Further 208 conformations were generated from metadynamics simulation whereby the CV was defined as the separation between the gold atom and one of the top aluminum atoms. The ML-PES was trained using PaiNN with a RMSE of 19 meV per conformation for the test set (10% of the overall 18471 reference conformations).

Figure 5A shows the diffusion potential of the gold atom computed by nudged elastic band (NEB) method between two hollow positions via the bridge position as transition state. The solid blue line and dashed red line show the minimum energy path (MEP) computed by the PBE/PAW reference method and trained model potential, respectively. With a reference diffusion barrier of 0.67 eV (solid blue line at TS) the model potential predicts 0.71 eV for the same conformation (dashed purple line at TS). The diffusion barrier in the MEP obtained by the model potential is 0.69 eV (dashed red line at TS).

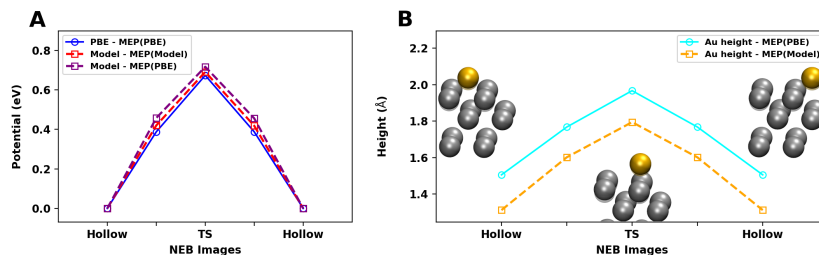


Figure 5: Panel A: Minimum energy path (MEP) for a gold atom diffusion on Al(100) surface (hollow \rightarrow bridge \rightarrow hollow) computed by NEB simulation using PBE/PAW level of theory (blue marker) and a PaiNN model potential (red marker) trained on Au/Al(100) reference data set. The purple line shows the energy prediction of the PaiNN model potential along the MEP structures from NEB with PBE/PAW. Panel B shows the Au atom height from the ideal surface layer height and sketches of MEP.

Even though the diffusion barrier prediction in the model MEP is close to the one of the reference MEP, the surface height of the gold atom shown in Figure 5B is predicted to be about 0.17 \AA lower in the model MEP than in the reference MEP. The reason is a qualitatively structural wrong equilibrium position of the gold atom on the hollow site of Al(100). Such deficiency must be corrected by, e.g., adaptive sampling of the PaiNN model potential before it can be used for accurate predictions. However, the example shows the capability of Asparagus to handle periodic systems including all functionalities also available for non-periodic systems.

5. Conclusions

This work introduces the Asparagus workflow which supports a largely autonomous construction of ML-PESs starting from a (few) molecular structures. The pipeline starts with different implemented sampling methods, already existing datasets or other strategies to obtain reference conformation for which, supported by Asparagus, the reference properties can be computed with *ab-initio* codes. Next, Asparagus handles the generated data and makes them available for ML model training in a Asparagus style database file. Asparagus also shows the statistical model performance metric in publication quality graphs (c.f. Figure 4A). At present, two popular atomistic NN models, PhysNet and PaiNN, are available. Once the obtained

ML-PES is of the desired quality, *Asparagus* provides tools for characterising the PES such as the calculation of MEP, MDP, DMC, or harmonic frequencies. On the application-driven side, *Asparagus* includes interfaces to ASE and pyCHARMM, allowing the use of the generated potentials for running MD simulations.

Asparagus provides a comprehensive workflow for autonomous construction, validation, and use of ML-PESs. This considerably lowers technical barriers increasing the confidence in model quality and supporting workflow reproducibility, as well as the long-term availability of the model generation pipeline. *Asparagus* is an open project that will allow further improvements and incorporation of the latest advances in the field of ML potentials models. Future extensions include uncertainty quantification,[83] active learning, automatization of transfer learning procedures, and interfaces to other established MD codes such as LAMMPS.[34]

Acknowledgments

The authors gratefully acknowledge financial support from the Swiss National Science Foundation through grants 200020_219779, 200021_215088, the NCCR-MUST, the AFOSR and the European Union’s Horizon 2020 research and innovation program under the Marie Skłodowska-Curie grant agreement No 801459 -FP-RESOMUS. LIVS acknowledges funding from the Swiss National Science Foundation (Grant P500PN_222297). The authors thank Dr. Silvan Käser for providing the implementation regarding the computation of the Minimum Dynamic Path and the Diffusion Monte Carlo method. The authors also acknowledge Kartheek Sivasubramaniam and Timon Eya for the initial tests of the code and members of the Meuwly group for helpful discussions and testing.

References

- [1] P. L. Houston, C. Qu, Q. Yu, R. Conte, A. Nandi, J. K. Li, J. M. Bowman, PESPIP: Software to fit complex molecular and many-body potential energy surfaces with permutationally invariant polynomials, *J. Chem. Phys.* 158 (4), 044109 (2023).

- [2] B. J. Braams, J. M. Bowman, Permutationally invariant potential energy surfaces in high dimensionality, *Intern. Rev. Phys. Chem.* 28 (4) (2009) 577–606.
- [3] K. T. Schuett, H. E. Sauceda, P. J. Kindermans, A. Tkatchenko, K. R. Mueller, Schnet - a deep learning architecture for molecules and materials, *J. Chem. Phys.* 148 (24) (2018) 241722.
- [4] O. T. Unke, M. Meuwly, Physnet: A neural network for predicting energies, forces, dipole moments, and partial charges, *J. Chem. Theory Comput.* 15 (6) (2019) 3678–3693.
- [5] X. Zheng, P. Zheng, R.-Z. Zhang, Machine learning material properties from the periodic table using convolutional neural networks, *Chem. Sci.* 9 (2018) 8426–8432.
- [6] S. Chmiela, A. Tkatchenko, H. E. Sauceda, I. Poltavsky, K. T. Schütt, K.-R. Müller, Machine learning of accurate energy-conserving molecular force fields, *Sci. Adv.* 3 (5) (2017) e1603015.
- [7] H. E. Sauceda, S. Chmiela, I. Poltavsky, K.-R. Müller, A. Tkatchenko, Molecular force fields with gradient-domain machine learning: Construction and application to dynamics of small molecules with coupled cluster forces, *J. Chem. Phys.* 150 (11) (2019) 114102.
- [8] T.-S. Ho, H. Rabitz, A general method for constructing multidimensional molecular potential energy surfaces from *ab initio* calculations, *J. Chem. Phys.* 104 (7) (1996) 2584–2597.
- [9] T. Hollebeek, T.-S. Ho, H. Rabitz, Constructing multidimensional molecular potential energy surfaces from *ab initio* data, *Ann. Rev. Phys. Chem.* 50 (1) (1999) 537–570.
- [10] O. T. Unke, M. Meuwly, Toolkit for the construction of reproducing kernel-based representations of data: Application to multidimensional potential energy surfaces, *J. Chem. Inf. and Mod.* 57 (8) (2017) 1923–1931.
- [11] A. S. Christensen, L. A. Bratholm, F. A. Faber, O. Anatole von Lilienfeld, Fchl revisited: Faster and more accurate quantum machine learning, *J. Chem. Phys.* 152 (4) (2020) 044107.

- [12] A. P. Bartók, M. C. Payne, R. Kondor, G. Csányi, Gaussian approximation potentials: The accuracy of quantum mechanics, without the electrons, *Phys. Rev. Lett.* 104 (13) (2010) 136403.
- [13] J. Cui, R. V. Krems, Efficient non-parametric fitting of potential energy surfaces for polyatomic molecules with Gaussian processes, *J. Phys. B: Atom. Mol. Opt. Phys.* 49 (22) (2016) 224001.
- [14] O. T. Unke, S. Chmiela, H. E. Sauceda, M. Gastegger, I. Poltavsky, K. T. Schütt, A. Tkatchenko, K.-R. Müller, Machine learning force fields, *Chem. Rev.* 121 (16) (2021) 10142–10186.
- [15] S. Manzhos, T. Carrington Jr, Neural network potential energy surfaces for small molecules and reactions, *Chem. Rev.* 121 (16) (2021) 10187–10217.
- [16] M. Meuwly, Machine learning for chemical reactions, *Chem. Rev.* 121 (16) (2021) 10218–10239.
- [17] V. L. Deringer, A. P. Bartók, N. Bernstein, D. M. Wilkins, M. Ceriotti, G. Csányi, Gaussian process regression for materials and molecules, *Chem. Rev.* 121 (16) (2021) 10073–10141.
- [18] O. T. Unke, S. Chmiela, H. E. Sauceda, M. Gastegger, I. Poltavsky, K. T. Schütt, A. Tkatchenko, K.-R. Müller, Machine learning force fields, *Chem. Rev.* 121 (16) (2021) 10142–10186.
- [19] C. Qu, R. Conte, P. L. Houston, J. M. Bowman, Full-dimensional potential energy surface for acetylacetone and tunneling splittings, *Phys. Chem. Chem. Phys.* 23 (13) (2021) 7758–7767.
- [20] S. Käser, J. O. Richardson, M. Meuwly, Transfer learning for affordable and high-quality tunneling splittings from instanton calculations, *J. Chem. Theory Comput.* 18 (11) (2022) 6840–6850.
- [21] A. Warshel, R. M. Weiss, An empirical valence bond approach for comparing reactions in solutions and in enzymes, *J. Am. Chem. Soc.* 102 (20) (1980) 6218–6226.
- [22] T. Nagy, J. Yosa Reyes, M. Meuwly, Multisurface adiabatic reactive molecular dynamics, *J. Chem. Theory Comput.* 10 (4) (2014) 1366–1375.

- [23] A. C. Van Duin, S. Dasgupta, F. Lorant, W. A. Goddard, Reaxff: a reactive force field for hydrocarbons, *J. Phys. Chem. A* 105 (41) (2001) 9396–9409.
- [24] F. Jensen, *Introduction to computational chemistry*, John Wiley & Sons, 2017.
- [25] M. Pinheiro Jr, P. O. Dral, Kernel methods, in: *Quantum Chemistry in the Age of Machine Learning*, Elsevier, 2023, pp. 205–232.
- [26] X. Gao, F. Ramezanghorbani, O. Isayev, J. S. Smith, A. E. Roitberg, TorchANI: a free and open source PyTorch-based deep learning implementation of the ANI neural network potentials, *J. Chem. Inf. and Mod.* 60 (7) (2020) 3408–3415.
- [27] S. Doerr, M. Majewski, A. Pérez, A. Kramer, C. Clementi, F. Noe, T. Giorgino, G. De Fabritiis, Torchmd: A deep learning framework for molecular simulations, *J. Chem. Theory Comput.* 17 (4) (2021) 2355–2363.
- [28] K. T. Schütt, S. S. Hessmann, N. W. Gebauer, J. Lederer, M. Gastegger, Schnetpack 2.0: A neural network toolbox for atomistic machine learning, *J. Chem. Phys.* 158 (14) (2023).
- [29] T. Plé, O. Adjoua, L. Lagardère, J.-P. Piquemal, Fennol: an efficient and flexible library for building force-field-enhanced neural network potentials, *arXiv preprint arXiv:2405.01491* (2024).
- [30] P. O. Dral, F. Ge, Y.-F. Hou, P. Zheng, Y. Chen, M. Barbatti, O. Isayev, C. Wang, B.-X. Xue, M. Pinheiro Jr, et al., MLatom 3: A platform for machine learning-enhanced computational chemistry simulations and workflows, *J. Chem. Theory Comput.* 20 (3) (2024) 1193–1213.
- [31] H. Wang, L. Zhang, J. Han, E. Weinan, DeePMD-kit: A deep learning package for many-body potential energy representation and molecular dynamics, *Comput. Phys. Commun.* 228 (2018) 178–184.
- [32] J. Zeng, D. Zhang, D. Lu, P. Mo, Z. Li, Y. Chen, M. Rynik, L. Huang, Z. Li, S. Shi, et al., DeePMD-kit v2: A software package for deep potential models, *J. Chem. Phys.* 159 (5) (2023).

- [33] A. H. Larsen, J. J. Mortensen, J. Blomqvist, I. E. Castelli, R. Christensen, M. Dulak, J. Friis, M. N. Groves, B. Hammer, C. Hargus, et al., The atomic simulation environment—a python library for working with atoms, *J. Phys. Condens. Matter* 29 (27) (2017) 273002.
- [34] A. P. Thompson, H. M. Aktulga, R. Berger, D. S. Bolintineanu, W. M. Brown, P. S. Crozier, P. J. in 't Veld, A. Kohlmeyer, S. G. Moore, T. D. Nguyen, R. Shan, M. J. Stevens, J. Tranchida, C. Trott, S. J. Plimpton, LAMMPS - a flexible simulation tool for particle-based materials modeling at the atomic, meso, and continuum scales, *Comp. Phys. Comm.* 271 (2022) 108171.
- [35] R. David, M. de la Puente, A. Gomez, O. Anton, G. Stirnemann, D. Laage, ArcaNN: automated enhanced sampling generation of training sets for chemically reactive machine learning interatomic potentials, *arXiv preprint arXiv:2407.07751* (2024). [arXiv:2407.07751](https://arxiv.org/abs/2407.07751).
- [36] J. Buckner, X. Liu, A. Chakravorty, Y. Wu, L. F. Cervantes, T. T. Lai, C. L. Brooks III, pyCHARMM: Embedding CHARMM functionality in a python framework, *J. Chem. Theory Comput.* 19 (12) (2023) 3752–3762.
- [37] K. Song, S. Käser, K. Töpfer, L. I. Vazquez-Salazar, M. Meuwly, Phys-Net meets CHARMM: A framework for routine machine learning/molecular mechanics simulations, *J. Chem. Phys.* 159 (2) (2023) 024125.
- [38] A. Paszke, S. Gross, F. Massa, A. Lerer, J. Bradbury, G. Chanan, T. Killeen, Z. Lin, N. Gimelshein, L. Antiga, A. Desmaison, A. Kopf, E. Yang, Z. DeVito, M. Raison, A. Tejani, S. Chilamkurthy, B. Steiner, L. Fang, J. Bai, S. Chintala, Pytorch: An imperative style, high-performance deep learning library, in: *Adv. Neural Inf. Process. Syst.* 32, Curran Associates, Inc., 2019, pp. 8024–8035.
- [39] J. Behler, Four generations of high-dimensional neural network potentials, *Chem. Rev.* 121 (16) (2021) 10037–10072.
- [40] S. Käser, L. I. Vazquez-Salazar, M. Meuwly, K. Töpfer, Neural network potentials for chemistry: concepts, applications and prospects, *Digit. Discov.* 2 (1) (2023) 28–58.

- [41] F. Neese, F. Wennmohs, U. Becker, C. Riplinger, The ORCA quantum chemistry program package, *J. Chem. Phys.* 152 (22) (2020) 224108.
- [42] M. Frisch, G. Trucks, H. Schlegel, G. Scuseria, M. Robb, J. Cheeseman, G. Scalmani, V. Barone, G. Petersson, H. Nakatsuji, et al., *Gaussian 16* (2016).
- [43] O. T. Unke, M. Meuwly, Physnet: A neural network for predicting energies, forces, dipole moments, and partial charges, *J. Chem. Theory Comput.* 15 (6) (2019) 3678–3693.
- [44] K. Schütt, O. Unke, M. Gastegger, Equivariant message passing for the prediction of tensorial properties and molecular spectra, in: *International Conference on Machine Learning*, PMLR, 2021, pp. 9377–9388.
- [45] K. T. Schütt, H. E. Sauceda, P.-J. Kindermans, A. Tkatchenko, K.-R. Müller, Schnet—a deep learning architecture for molecules and materials, *J. Chem. Phys.* 148 (24) (2018) 241722.
- [46] S. Batzner, A. Musaelian, L. Sun, M. Geiger, J. P. Mailoa, M. Kornbluth, N. Molinari, T. E. Smidt, B. Kozinsky, E(3)-equivariant graph neural networks for data-efficient and accurate interatomic potentials, *Nat. Comm.* 13 (1) (2022) 2453.
- [47] I. Batatia, D. P. Kovacs, G. Simm, C. Ortner, G. Csányi, Mace: Higher order equivariant message passing neural networks for fast and accurate force fields, *Advances in Neural Information Processing Systems* 35 (2022) 11423–11436.
- [48] O. T. Unke, S. Brickel, M. Meuwly, Sampling reactive regions in phase space by following the minimum dynamic path, *J. Chem. Phys.* 150 (7) (2019).
- [49] I. Kosztin, B. Faber, K. Schulten, Introduction to the diffusion Monte Carlo method, *Am. J. Phys.* 64 (5) (1996) 633–644.
- [50] J. Li, C. Qu, J. M. Bowman, Diffusion Monte Carlo with fictitious masses finds holes in potential energy surfaces, *Mol. Phys.* 119 (17-18) (2021) e1976426.

- [51] R. Conte, P. L. Houston, C. Qu, J. Li, J. M. Bowman, Full-dimensional, ab initio potential energy surface for glycine with characterization of stationary points and zero-point energy calculations by means of diffusion Monte Carlo and semiclassical dynamics, *J. Chem. Phys.* 153 (24) (2020) 244301.
- [52] S. Käser, M. Meuwly, Transfer learned potential energy surfaces: accurate anharmonic vibrational dynamics and dissociation energies for the formic acid monomer and dimer, *Phys. Chem. Chem. Phys.* 24 (9) (2022) 5269–5281.
- [53] B. R. Brooks, C. L. Brooks III, A. D. MacKerell Jr., L. Nilsson, R. J. Petrella, B. Roux, Y. Won, G. Archontis, C. Bartels, S. Boresch, A. Caffisch, L. Caves, Q. Cui, A. R. Dinner, M. Feig, S. Fischer, J. Gao, M. Hodoscek, W. Im, K. Kuczera, T. Lazaridis, J. Ma, V. Ovchinnikov, E. Paci, E. W. Pastor, J. Z. Post, C. B. andPu, M. Schaefer, B. Tidor, R. M. Venable, H. L. Woodcock, X. Wu, W. Yang, D. M. York, M. Karplus, CHARMM: The biomolecular simulation program, *J. Comput. Chem.* 30 (2009) 1545–1614.
- [54] K. Vanommeslaeghe, E. Hatcher, C. Acharya, S. Kundu, S. Zhong, J. Shim, E. Darian, O. Guvench, P. Lopes, I. Vorobyov, A. D. Mackerell Jr., CHARMM general force field: A force field for drug-like molecules compatible with the CHARMM all-atom additive biological force fields, *J. Comput. Chem.* 31 (4) (2010) 671–690.
- [55] K. Töpfer, S. Käser, M. Meuwly, Double proton transfer in hydrated formic acid dimer: Interplay of spatial symmetry and solvent-generated force on reactivity, *Phys. Chem. Chem. Phys.* 24 (22) (2022) 13869–13882.
- [56] G. Henkelman, G. Jóhannesson, H. Jónsson, *Methods for finding saddle points and minimum energy paths*, Springer, 2002, pp. 269–302.
- [57] M. Krummenacher, M. Gubler, J. A. Finkler, H. Huber, M. Sommer-Jørgensen, S. Goedecker, Performing highly efficient minima hopping structure predictions using the atomic simulation environment (ase), *SoftwareX* 25 (2024) 101632.

- [58] D. J. Wales, J. P. Doye, Global optimization by basin-hopping and the lowest energy structures of lennard-jones clusters containing up to 110 atoms, *J. Phys. Chem. A* 101 (28) (1997) 5111–5116.
- [59] C. Bannwarth, S. Ehlert, S. Grimme, Gfn2-xtb—an accurate and broadly parametrized self-consistent tight-binding quantum chemical method with multipole electrostatics and density-dependent dispersion contributions, *J. Chem. Theory Comput.* 15 (3) (2019) 1652–1671.
- [60] H.-J. Werner, P. J. Knowles, G. Knizia, F. R. Manby, M. Schütz, et al., Molpro, version 2019.2, a package of ab initio programs (2019).
- [61] S. Chib, E. Greenberg, Understanding the metropolis-hastings algorithm, *The american statistician* 49 (4) (1995) 327–335.
- [62] N. Metropolis, A. W. Rosenbluth, M. N. Rosenbluth, A. H. Teller, E. Teller, Equation of state calculations by fast computing machines, *J. Chem. Phys.* 21 (6) (1953) 1087–1092.
- [63] J. S. Smith, O. Isayev, A. E. Roitberg, ANI-1: an extensible neural network potential with DFT accuracy at force field computational cost, *Chem. Sci.* 8 (4) (2017) 3192–3203.
- [64] K. Brezina, H. Beck, O. Marsalek, Reducing the cost of neural network potential generation for reactive molecular systems, *J. Chem. Theory Comput.* 19 (19) (2023) 6589–6604.
- [65] A. Laio, M. Parrinello, Escaping free-energy minima, *Proc. Natl. Acad. Sci. USA* 99 (20) (2002) 12562–12566.
- [66] G. Bussi, A. Laio, Using metadynamics to explore complex free-energy landscapes, *Nat. Rev. Phys* 2 (4) (2020) 200–212.
- [67] B. Peters, Reaction coordinates and mechanistic hypothesis tests, *Ann. Rev. Phys. Chem.* 67 (2016) 669–690.
- [68] J. E. Herr, K. Yao, R. McIntyre, D. W. Toth, J. Parkhill, Metadynamics for training neural network model chemistries: A competitive assessment, *J. Chem. Phys.* 148 (24) (2018) 241710.

- [69] J. Pfandtner, Metadynamics to enhance sampling in biomolecular simulations, in: *Biomolecular Simulations: Methods and Protocols*, Springer, 2019, pp. 179–200.
- [70] D. Yoo, J. Jung, W. Jeong, S. Han, Metadynamics sampling in atomic environment space for collecting training data for machine learning potentials, *NPJ Comput. Mater.* 7 (1) (2021) 131.
- [71] D. P. Kingma, J. Ba, Adam: A method for stochastic optimization, arXiv preprint arXiv:1412.6980 (2014).
- [72] S. J. Reddi, S. Kale, S. Kumar, On the convergence of adam and beyond, in: *International Conference on Learning Representations*, 2018.
URL <https://openreview.net/forum?id=ryQu7f-RZ>
- [73] L. Prechelt, Early stopping-but when?, in: *Neural Networks: Tricks of the trade*, Springer, 2002, pp. 55–69.
- [74] L. Verlet, Computer "experiments" on classical fluids. i. thermodynamical properties of Lennard-Jones molecules, *Phys. Rev.* 159 (1967) 98–103.
- [75] J. B. Anderson, A random-walk simulation of the Schrödinger equation: H_3^+ , *J. Chem. Phys.* 63 (4) (1975) 1499–1503.
- [76] M. Quack, M. A. Suhm, Potential energy surfaces, quasiadiabatic channels, rovibrational spectra, and intramolecular dynamics of $(HF)_2$ and its isotopomers from quantum Monte Carlo calculations, *J. Chem. Phys.* 95 (1) (1991) 28–59.
- [77] W. L. Jorgensen, J. Chandrasekhar, J. D. Madura, R. W. Impey, M. L. Klein, Comparison of simple potential functions for simulating liquid water, *J. Chem. Phys.* 79 (1983) 926–935.
- [78] J. Young, J. Osborn, F. Jardine, G. Wilkinson, Hydride intermediates in homogeneous hydrogenation reactions of olefins and acetylenes using rhodium catalysts, *Chem. Comm.* (7) (1965) 131–132.
- [79] P. van Gerwen, A. Fabrizio, M. D. Wodrich, C. Corminboeuf, Physics-based representations for machine learning properties of chemical reactions, *Mach. Learn.: Sci. Technol.* 3 (4) (2022) 045005.

- [80] J. J. Mortensen, A. H. Larsen, M. Kuisma, A. V. Ivanov, A. Taghizadeh, A. Peterson, A. Haldar, A. O. Dohn, C. Schäfer, E. Ö. Jónsson, et al., GPAW: An open python package for electronic structure calculations, *J. Chem. Phys.* 160 (9) (2024).
- [81] Surface diffusion energy barriers using the nudged elastic band (NEB) method, <https://wiki.fysik.dtu.dk/ase/tutorials/neb/diffusion.html>, accessed: 2024-07-09.
- [82] Diffusion of gold atom on Al(100) surface, <https://wiki.fysik.dtu.dk/gpaw/tutorialsexercises/moleculardynamics/diffusion/diffusion.html>, accessed: 2024-07-09.
- [83] L. I. Vazquez-Salazar, E. D. Boittier, M. Meuwly, Uncertainty quantification for predictions of atomistic neural networks, *Chem. Sci.* 13 (44) (2022) 13068–13084.